IEEE Access
Multidisciplinary | Rapid Review | Open Access Journal

Received May 1, 2021, accepted May 16, 2021, date of publication May 25, 2021, date of current version June 8, 2021.

Digital Object Identifier 10.1109/ACCESS.2021.3083498

Fast 3D-HEVC Depth Intra Coding Based on Boundary Continuity

MEI-JUAN CHEN[1], (Senior Member, IEEE), JIE-RU LIN[1], YU-CHIH HSU[1], YI-SHENG CIOU[1], CHIA-HUNG YEH[2,3], (Senior Member, IEEE), MIN-HUI LIN[3], LIH-JEN KAU[4], (Senior Member, IEEE), AND CHUAN-YU CHANG[5], (Senior Member, IEEE)

[1]Department of Electrical Engineering, National Dong Hwa University, Hualien 974301, Taiwan
[2]Department of Electrical Engineering, National Taiwan Normal University, Taipei 106010, Taiwan
[3]Department of Electrical Engineering, National Sun Yat-sen University, Kaohsiung 804201, Taiwan
[4]Department of Electronic Engineering, National Taipei University of Technology, Taipei 106344, Taiwan
[5]Department of Computer Science and Information Engineering, National Yunlin University of Science and Technology, Yunlin 640301, Taiwan

Corresponding author: Chia-Hung Yeh (chyeh@ntnu.edu.tw)

This work was supported by the Ministry of Science and Technology, Taiwan, under Grant MOST 103-2221-E-259-009-MY3 and Grant MOST 106-2221-E-259-009-MY3.

ABSTRACT The encoding format of the 3D extension of high efficiency video coding (3D-HEVC) consists of a multiview color texture and an associated depth map. Because of the unique characteristics of the depth map, advanced coding techniques are designed for depth map coding at the expense of computational complexity. In this paper, fast algorithms are conceived to accelerate the intra coding time of the depth map based on boundary continuity. First, the proposed fast prediction unit (PU) mode decision reduces the number of conventional intra prediction modes based on calculating the total sum of squares (TSS) of the PU boundaries. Second, the proposed fast depth modeling mode (DMM) decision makes use of the variances of the boundary pixels to determine the execution of the DMM. Third, the proposed coding unit (CU) early termination algorithm decides whether to further split the current CU by utilizing the thresholds of the TSS and the rate-distortion cost (RD-cost). The experimental results show that the proposed algorithm provides better performance in terms of coding speed and bitrate than the algorithm in previous work. The coding time of the depth map is reduced by 56.08%, while the Bjøntegaard delta bitrate (BD-BR) is only increased by 0.32% for the synthesis view.

INDEX TERMS 3D-HEVC, depth map, intra coding, fast algorithm, boundary continuity.

I. INTRODUCTION

With the requirement of video applications, video technology has become increasingly advanced in recent years. 3D videos have the ability to provide users with fantastic experiences in a stereoscopic world. The 3D extension of high efficiency video coding (3D-HEVC) [1], [2] is the newest coding standard for encoding 3D videos effectively. The video format of the 3D-HEVC encoder is multiview plus depth (MVD) [3]–[5]. 3D-HEVC is based on the quad-tree coding architecture of high efficiency video coding (HEVC), which comprises coding tree units (CTUs) with coding units (CUs), prediction units (PUs), and transformation units (TUs). HEVC is designed basically for texture coding. However, the depth map in the 3D-HEVC system has some features, such as large amounts of smooth regions and sharp edges, which are totally different from each other in terms of color texture. Therefore, the conventional HEVC encoders may not always maintain good coding efficiency when encoding depth maps that consist of smooth regions or edges. For this reason, new coding tools have been created for depth map coding, such as the depth modeling mode (DMM) [6] and depth intra skip (DIS) [7]. The DMM in 3D-HEVC is intended to enhance the conventional intra coding by keeping the edge information and smoothing the unimportant regions. Fig.1 illustrates the system structure of 3D-HEVC [8].

Along with the evolution of the reference software, two DMM modes (DMM1 and DMM4) also evolved with the latest version of the 3D-HEVC encoder [8]. DMM1 is a Wedgelet partition while DMM4 is a contour partition. DMM1 (Wedgelet partition) uses a straight line to separate two regions, as shown in Fig. 2, where each region is

The associate editor coordinating the review of this manuscript and approving it for publication was Charith Abhayaratne.

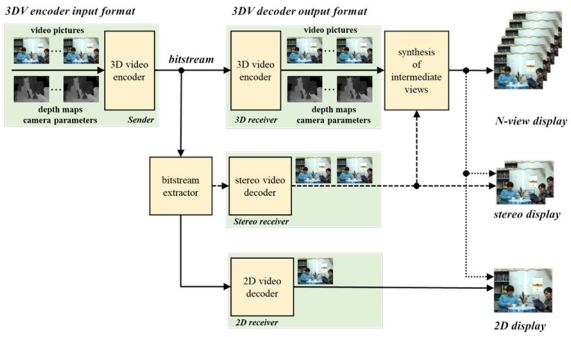

FIGURE 1. System structure for 3D-HEVC [8].

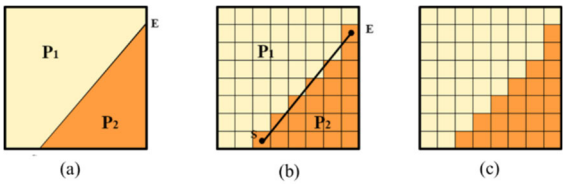

FIGURE 2. The Wedgelet partition of DMM1 [8].

represented by a constant value. Rather than checking the total Wedgelet partitions, the best Wedgelet partition mode is evaluated by estimating part of the possible cases with the refinement candidates. DMM4 (contour partition) divides the regions into two areas and represents each region with the same value by the threshold from the pixel values in the collocated texture block. The contour partition pattern is illustrated in Fig. 3. In addition, there are also several new coding tools for depth map coding. Segment-wise depth coding (SDC) represents the residual signal with a constant pixel value and replaces the traditional quantized discrete cosine transformation. Depth maps contain information for view synthesis rather than direct displays, so the original rate-distortion optimization (RDO) [9] method may not always be efficient for depth maps. View synthesis optimization (VSO) can take the quality of synthesized views into consideration during the calculation of RDO to improve depth map coding. In addition, several studies investigated how to further improve the compression efficiency or 3D video quality. Zhang *et al.* [10] proposed a full reference synthesized video quality metric and minimized the perceptual quality loss of the synthesized view by improving the RDO approach. Zhu *et al.* [11] conceived a convolutional neural network (CNN)-based VSO to elevate the coding performance. Shahriyar *et al.* [12] developed an independent depth map encoder with restricted quantization and proposed binary tree-based decomposition.

The flowchart of the intra prediction of the depth map is demonstrated in Fig. 4. The conventional intra prediction performs a rough mode decision (RMD) from the planar mode, the DC mode and 33 kinds of angular modes to obtain the intra mode candidates. Then, the most probable modes (MPM) are added. Finally, DMMs are carried out and inserted into the candidate list for rate-distortion optimization (RDO). The unique encoding techniques for

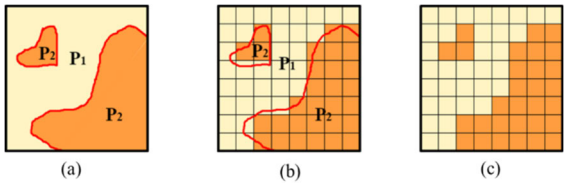

FIGURE 3. The contour partition of DMM4 [8].

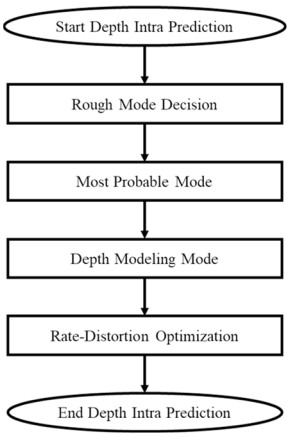

FIGURE 4. The flowchart of the intra prediction on depth map.

depth maps contribute to the enhancement of the compression efficiency. However, the complicated encoding procedures in 3D-HEVC increase the coding complexity and coding time. Researchers have dedicated themselves to simplifying the encoder or reducing the depth coding time. Chung *et al.* [13] proposed a bitrate-savings scheme with a no-synthesis-error model and terminated the quad-tree coding structure early. Lei *et al.* [14] employed grayscale similarity of the depth map as well as interview dependency to perform a fast mode decision. Shen *et al.* [15] classified the CU complexity by weighting the intercomponent, interview and spatiotemporal coding information to select the corresponding intra prediction modes. Hamout and Elyousfi [16] simplified depth intra coding by extracting tensor features and data clustering. Sanchez *et al.* [17] found the positions of the eight highest gradients among the PU boundaries. Only DMMs with a start point or an end point passing through these positions were executed. Sanchez *et al.* [18] proposed the strong gradient-based mode one filter (S-GMOF) to detect the two boundaries with the highest gradients. If the start point and end point of the DMM1 partition were located at the two boundaries, the DMMs were executed. Otherwise, the modes in DMM 1 were ignored. Saldanha *et al.* [19] proposed single degree of freedom GMOF (SDF-GMOF) and double degree of freedom GMOF (DDF-GMOF) to quickly select the best positions to perform the prediction of DMM1. Fu *et al.* [20] separated the PU into two parts and defined the directions into four classes, including vertical, horizontal, and two diagonal (45° and 135°) directions. Then, the number of DMMs was reduced according to the variance and the direction. By using the correlation between the current PU and parent

PUs, Zhang *et al.* [21] reduced the number of intra modes during RMD and determined whether to implement SDC. Hong *et al.* [22] analyzed the rate-distortion cost (RD-cost) distributions of both rough mode decisions and DMMs with the one-sided Chebyshev's inequality to decide the adjustable threshold for early termination. Gu *et al.* [23] analyzed the RD-cost of the RMD to estimate a threshold for the early termination of the following intra modes. Park [24] selectively skipped the unrelated partition of DMM1 by classifying the edge orientation of a PU. Zhang *et al.* [25] evaluated the smoothness of the current CU to bypass the DMM decision by referencing the collocated CU in the depth map and the corresponding CU in the color texture. Zhang *et al.* [26] replaced the view synthesis distortion (VSD)-based VSO with the proposed squared Euclidean distance of variances (SEDV) to diminish the complexity of the DMM1 prediction. In addition, the probability-based early depth intra mode decision (PBED) in [26] skipped the DMM prediction and chose SDC as the only candidate for RDO if the minimum RD-cost of the RMD candidates was smaller than the threshold. Saldanha *et al.* [27] used specialized decision trees for I-frames, P-frames and B-frames to define 64×64, 32×32, and 16×16 partitions. The characteristics of the human visual system were utilized in [28] to propose a fast algorithm based on visual perceptions for fast depth intra coding of 3D-HEVC. Shen *et al.* [29] designed an edge-aware prediction scheme to reduce the prediction error energy in blocks with arbitrary edge shapes and thus decrease the bitrate for the depth map. Shen *et al.* [30] presented a new set of edge-adaptive transforms as an alternative to the standard discrete cosine transform to provide significant bitrate reductions for depth map coding. Important contributions were made by [31]—[33] to intra predictions when edges are found. Our previous works [34]–[36] also contributed to the reduction of the depth coding time. In [34], we defined a tunable threshold based on boundary variance and proposed a fast DMM decision scheme. In [35], we terminated the CU partition early based on the total sum of squares to accelerate depth intra coding. Fast intra mode selection [36] was conceived to rapidly extract the intra prediction modes according to the total sum of squares. A complete framework is unified in this paper, which jointly considers coding properties at the CU and PU levels. In addition, more analysis and validation are provided to justify the proposed algorithm.

Table 1 tabulates the coding performance of Bjøntegaard delta bitrate (BD-BR) and time saving (TS) with disabled DMMs. We know that the DMM evidently occupies the coding time and affects coding efficiency. Most of the previous works proposed fast DMM decisions to reduce the coding time and minimize the BD-BR loss. However, under the all-intra configuration, the computational time consumption of DMMs only accounts for 24.8% of the overall coding time, as shown in Table 1, whereas the depth coding time accounts for 86% for the all-intra configuration, as shown in Fig. 5. Consequently, depth coding time savings should be improved. In this paper, we propose three fast algorithms

TABLE 1. BD-BR and time-saving performance of the synthesized view with DMM disabled.

Sequence	BD-BR(%)	TS(%)
Kendo	2.25	25.6
Balloons	7.56	27.4
Newspaper	9.65	29.8
Poznan_Street	1.95	25.0
Poznan_Hall2	8.53	18.5
Shark	6.58	25.5
Undo_Dancer	7.80	21.8
GT_Fly	2.66	25.1
Average	**5.87**	**24.8**

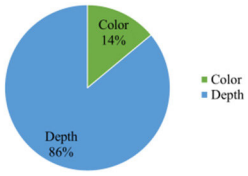

FIGURE 5. Coding time distribution of color texture and depth map under all-intra configuration.

based on boundary continuity checks to accelerate the encoding procedures of depth intra coding. First, at the prediction unit (PU) level, we abridge the number of intra angular modes and shrink the candidates for RMD. Second, the proposed fast DMM decision determines whether to execute DMM prediction by investigating the variance of each boundary and detecting whether there is an edge passing through it. Third, at the CU level, the CU early termination scheme is designed by inspecting the overall total sum of squares (TSS) of a CU and combining the limitation of the RD-cost.

II. PROPOSED METHOD

A. OBSERVATIONS FROM THE DEPTH MAP

Fig. 6 illustrates the depth map of the Shark sequence. Apparently, there exists a large quantity of sharp edges (blue squares in Fig. 6) and smooth areas (red squares in Fig. 6) within the depth map. Sharp edges are very likely to traverse the boundaries of the coding blocks. Studies also indicate that 3D-HEVC is prone to encode smooth areas with larger CU sizes. In this paper, we detect whether there is an edge passing

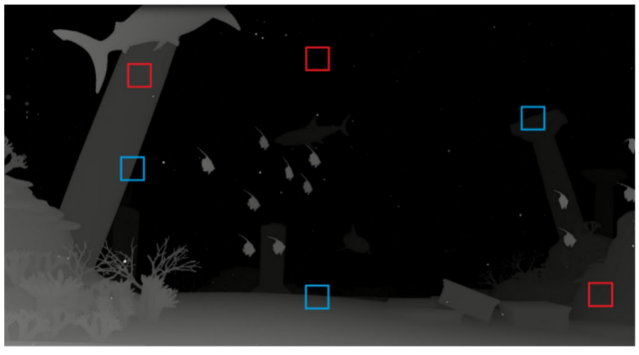

FIGURE 6. The depth map of the Shark sequence.

through the current coding block based on the boundary continuity. Further CU depths without any edge are terminated early. Additionally, the intra prediction modes and DMMs are conditionally skipped to accelerate the depth map coding.

B. FAST INTRA MODE DECISION

For blocks with smooth contents, planar mode, DC mode, vertical mode and horizontal mode are most likely to be encoded as the best intra mode. Accordingly, pruning the number of intra prediction modes and the number of rough mode decision (RMD) candidates may contribute to coding time reductions.

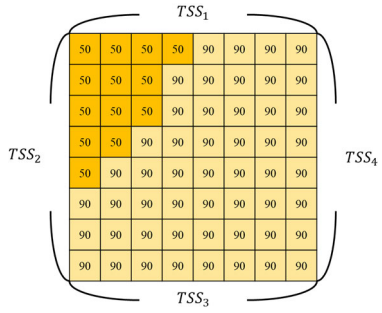

FIGURE 7. Illustration of the TSS calculation.

1) ESTIMATION OF THE BOUNDARY COMPLEXITY

First, we aim to identify the smoothness. A general case of a sharp edge in the depth map is illustrated in Fig. 7. Sharp edges are formed by an obvious gap in pixel variation. In addition, the edge extends, so an obvious pixel variation gap also appears at the block boundary. Along with these properties, in this paper, we calculate the total sum of the squares (TSS) of each boundary by (1)-(2) to analyze the boundary complexity. TSS_k symbolizes the total sum of the squares on the k-th boundary. $pix_{k,i}$, $pix_{k,avg}$ and w denote the i-th pixel value, the average pixel value on the k-th boundary and the width of the current PU, respectively. Supposing that the values of TSS_k for each boundary are all less than or equal to a threshold (Th_{TSS}), as described in (3), there is probably no edge passing through, and the current coding PU is less complicated. Instead of searching all 35 intra modes, we may only perform planar, DC, vertical, and horizontal modes, which are frequently the best intra modes. The number of RMD candidates is reduced from 8 to 3 when the PU sizes are 8×8 and 4×4. The flowchart of the fast intra mode decision is presented in Fig. 8.

$$TSS_k = \sum_{i=1}^{w} \left(pix_{k,i} - pix_{k,avg}\right)^2, \ k \in \{1, 2, 3, 4\} \quad (1)$$

$$pix_{k,avg} = \frac{1}{w} \sum_{i=1}^{w} pix_{k,i}, \quad k \in \{1, 2, 3, 4\} \quad (2)$$

$$TSS_k \leq Th_{TSS}, \quad k \in \{1, 2, 3, 4\} \quad (3)$$

2) ANALYSIS AND SELECTION OF Th_{TSS}

To select a suitable threshold, we encode 100 frames for the Ponzan_Street sequence with five Th_{TSS} values (0, 250, 500, 750, and 1000) and analyze the interaction between the depth coding time and the BD-BR performance of the synthesized view. Fig. 9 shows the statistical data of the Poznan_Street sequence. From the observation, the encoding time decreases as the threshold increases. However, the larger the threshold is, the more significant the BD-BR degradation. We find that when the thresholds are larger than 250, the encoding time becomes stable, whereas the BD-BR continues to rise dramatically. The saturation point of the encoding time is approximately 250. To balance the coding time reduction and coding efficiency, we set Th_{TSS} to 250. When Th_{TSS} is set to 250 and the quantization parameter (QP) is set to 30, the hit-rate of the PU mode, which is correctly selected as a DC, planar, horizontal or vertical mode, achieves 95.51% on average and at least 91.94%, as shown in Table 2, which validates the threshold selection.

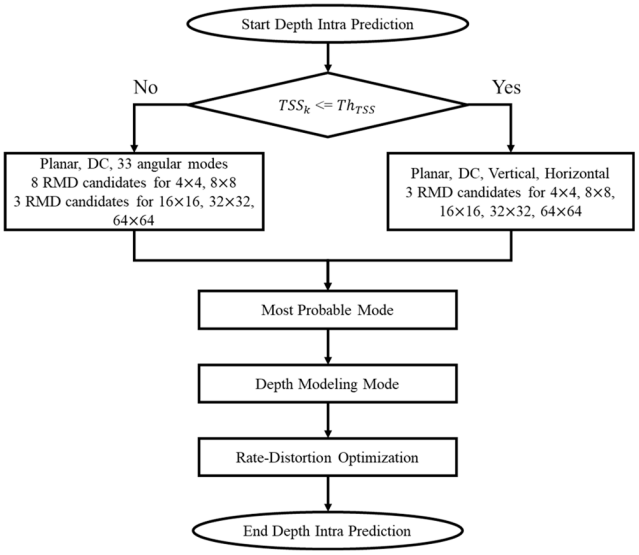

FIGURE 8. The flowchart of the proposed fast intra mode decision.

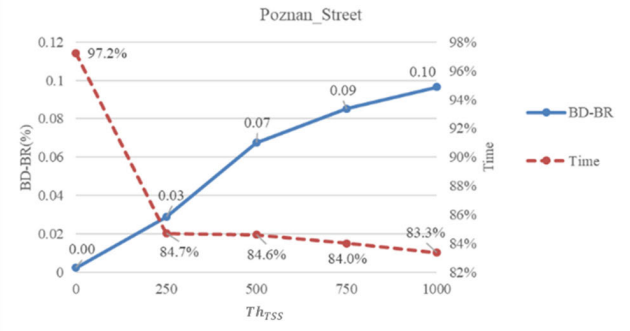

FIGURE 9. Coding performance under various values of Th_{TSS} for the Poznan_Street sequence.

C. FAST DMM DECISION

With the evolution of the HTM encoder, DMM1 partition types are simplified from approximately 1000 kinds to 500 kinds. The simplified DMM and built-in fast criterion decrease the DMM execution time. However, according to

TABLE 2. Hit-rate of PU mode selected as a DC, planar, horizontal or vertical mode when Th_{TSS} is set to 250 and QP is set to 30.

Sequence	Hit-rate (%)
Kendo	96.69
Balloons	94.85
Newspaper	92.43
Poznan_Street	96.05
Poznan_Hall2	98.99
Shark	91.94
Undo_Dancer	98.04
GT_Fly	95.12
Average	**95.51**

the analysis in [26], the DMM still occupies approximately 20.25% of the depth coding time, as shown in Fig. 10. As a result, we consider that a fast DMM decision is desired to accelerate coding.

1) FAST DMM DECISION BASED ON BOUNDARY VARIANCE

The principle of DMM1 is separating a PU into two regions by a straight line and predicting each region with a single value. In other words, DMM1 is designed particularly for a PU with any edge dividing two smooth areas. As a result, if the current coding PU selects the DMM as the best mode, there is probably an edge passing through it. In the proposed fast DMM decision, we detect the edge by calculating the boundary variance.

We calculate the variance of each boundary within the current PU and sort them from the largest to the smallest as formulated in (4). *Var* is the set that includes the ordered variances of the k-th boundary (Var_k). Equations (5) and (6) formulate the calculation of Var_k. w is the boundary width, $Pix_{k,i}$ denotes the i-th pixel value on the k-th boundary, and $Pix_{k,avg}$ is the average pixel value of the k-th boundary.

$$Var = \{Var_k | Var_1 \geq Var_2 \geq Var_3 \geq Var_4, k = 1 \; to \; 4\} \quad (4)$$

$$Var_k = \frac{1}{w}\sum_{i=1}^{w}(Pix_{k,i} - Pix_{k,avg})^2 \quad (5)$$

$$Pix_{k,avg} = \frac{1}{w}\sum_{i=1}^{w} Pix_{k,i} \quad (6)$$

$$(Var_1 + Var_2) - (Var_3 + Var_4) \leq Th_{var} \quad (7)$$

Among the four variances, Var_1 and Var_2 are denoted as the first two larger variances, while Var_3 and Var_4 are the other two smaller variances. Fig.11 illustrates an example of the four variances of the four boundaries. The difference between $(Var_1 + Var_2)$ and $(Var_3 + Var_4)$ is obvious, and the DMM is highly possible in this case. To confirm whether the boundaries are smooth enough or too complex to skip the DMM, we calculate the difference between $(Var_1 + Var_2)$ and $(Var_3 + Var_4)$ by (7) and check whether the difference is less than or equal to a threshold (Th_{var}). If the statement of (7) is true, the DMM will not be executed because it means that there may be no edge or the edges are too complicated and the DMM may not be suitable for this situation.

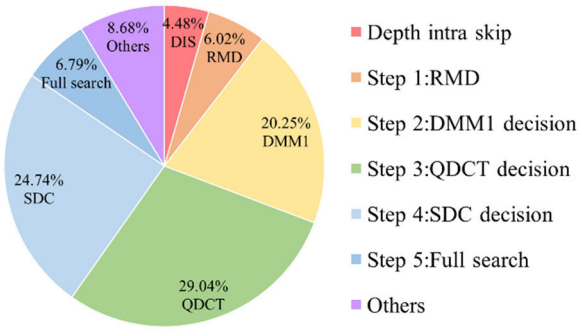

FIGURE 10. Coding time distribution of the depth map [26].

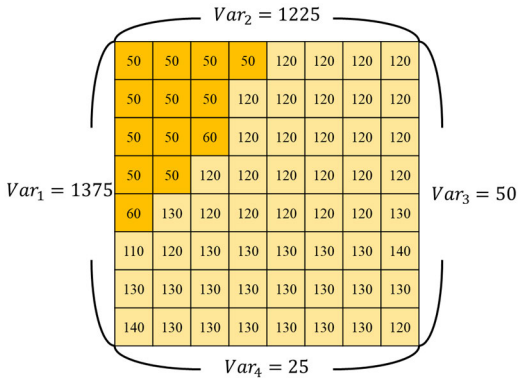

FIGURE 11. Illustration of boundary variation calculation.

2) ANALYSIS AND SELECTION OF Th_{var}

To analyze the performance of the proposed fast DMM decision under different values of $\boldsymbol{Th_{var}}$, we encode 100 frames of each benchmark sequence (Kendo, Balloons, Newspaper, Poznan_Street, Poznan_Hall2, Shark, Undo_Dancer, and GT_Fly) with various $\boldsymbol{Th_{var}}$ values (1, 2, 3, 5, 10, 20, 30, and 50). The interaction among the BD-BR of the synthesized view, depth coding time, and $\boldsymbol{Th_{var}}$ are plotted in Fig. 12. According to Fig. 12, the BD-BR degradation is still climbing, and the curve of the depth coding time becomes smooth when $\boldsymbol{Th_{var}}$ is approximately 20∼30. It seems that 20 or 30 is a suitable threshold value. However, we find that the BD-BR degrades too much when larger thresholds are used. To maintain the coding efficiency and avoid conflicts with other algorithms proposed by this paper, we decide to select a smaller threshold value. As a result, $\boldsymbol{Th_{var}}$ is set to 3 in this paper, and the flowchart of the proposed fast DMM decision is illustrated in Fig. 13.

D. FAST CU EARLY TERMINATION ALGORITHM WITH RD-COST LIMITATION

According to the analysis in [37], the encoding process of a CU depth of 0 only occupies 11.4% of the depth map coding time, as labeled in Fig. 14. In addition, CU depths of 1∼3

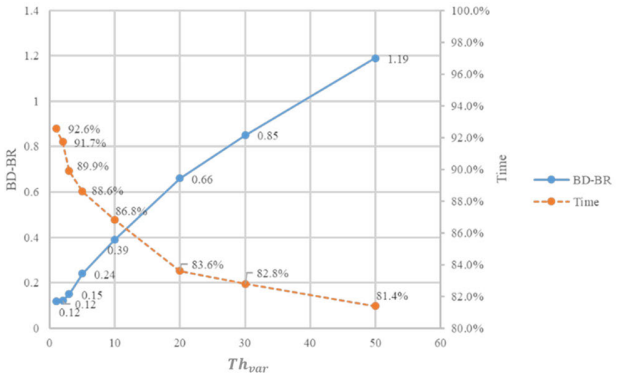

FIGURE 12. The interaction among BD-BR of the synthesized view, depth coding time, and Th_{var}.

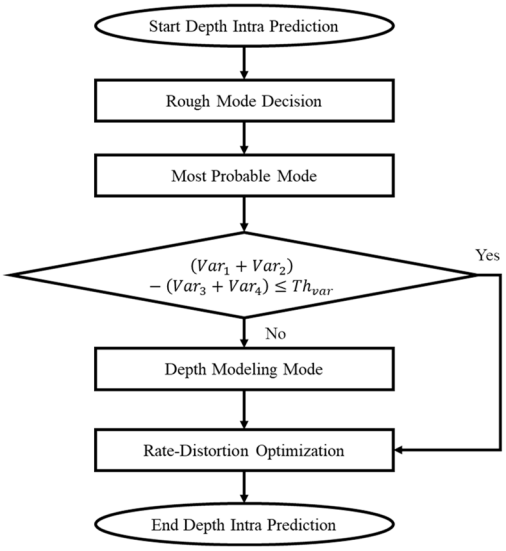

FIGURE 13. The flowchart of the proposed fast DMM decision.

accounted for 88.6% of the overall proportion. We further encode 100 frames for each benchmark sequence (Kendo, Balloons, Newspaper, Poznan_Street, Poznan_Hall2, Shark, Undo_Dancer, and GT_Fly) to estimate the probability distribution of each CU depth that is selected as the best CU depth, as shown in Fig. 15. Approximately 67.4% of the CTUs are partitioned at a depth of 0, whereas only 32.6% of the CTUs are split to CU depths of 1∼3. In other words, the original encoder consumes much coding time at CU depths of 1∼3, but most CTUs are partitioned at a CU depth of 0. Consequently, if we can determine the CU depth in advance and terminate the following CU encoding early, much time will be saved.

1) CU EARLY TERMINATION BASED ON TOTAL SUM OF SQUARES

The 3D-HEVC encoder is prone to select smooth areas with larger CU sizes. In other words, unnecessary partitioning at further CU splitting is likely to be bypassed to speed

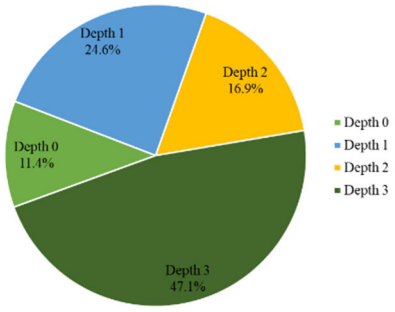

FIGURE 14. The encoding time distribution of the depth map at each CU depth under QP45 (Quantization parameter of 45) [37].

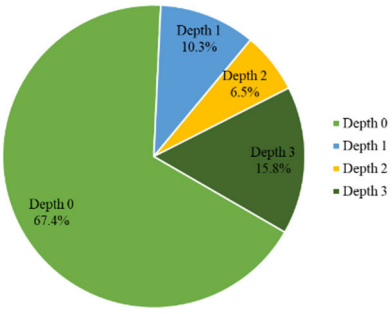

FIGURE 15. The probability distribution of each CU depth which is selected as the best CU depth.

up coding. First, we need to distinguish whether this area is smooth or if there is a complex edge. A sharp edge is formed by an obvious gap in pixel variation. In addition, the edge would extend, so an obvious pixel variation gap also appears at the block boundary. According to this observation, we calculate the TSS of each boundary (TSS_1, TSS_2, TSS_3, and TSS_4) of the CU to estimate the pixel variation as in (1) and find the TSS_{total} with (8). If TSS_{total} is less than or equal to the threshold (Th_{total}), there may be no edge passing through it. The block will be denoted as a smooth region, and further partitioning for smaller CU sizes will be terminated early.

$$TSS_{total} = \sum_{k=1}^{4} TSS_k \tag{8}$$

2) ANALYSIS AND SELECTION OF Th_{total}

To find an appropriate threshold, we encode 100 frames of each benchmark sequence (Kendo, Balloons, Poznan_Hall2, and GT_Fly) with various Th_{total} values (0, 500, 1000, 1500, 2000, and 2500). We analyze the tendency of coding time and the BD-BR performance under different settings of Th_{total}, as shown in Fig. 16. The larger Th_{total} is, the more CU partitions will be terminated early, and more coding time savings can be achieved. However, it is also accompanied by an increased BD-BR. The encoding time continues to decrease as Th_{total} and the BD-BR increase. When Th_{total} is approximately 1000, the curve of the coding time reduction

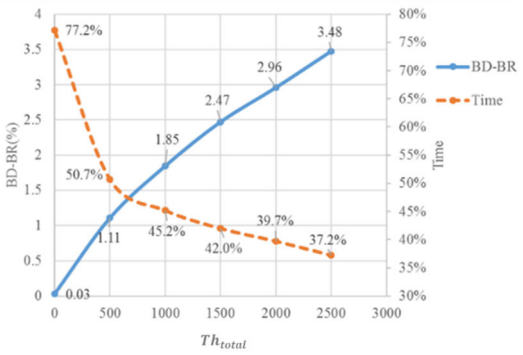

FIGURE 16. The interaction among BD-BR of the synthesized view, depth coding time and Th_{total}.

seems to be mitigated, and the BD-BR continues to degrade. Consequently, we set the Th_{total} to 1000.

3) THRESHOLD LIMITATION BASED ON THE RD-COST

Table 3 shows the detailed data of the BD-BR and TS performance when Th_{total} is set to 1000. We observe that the performance depends on the sequence, even though the average time saving is approximately 54.8% and the maximum time saving reaches 71.3%. For Poznan_Hall2, the BD-BR performance dramatically degrades to 5.21%, which means that this criterion is too rough to bring about the prediction error. Some kinds of CUs are smooth, but their RD-costs are extremely large, and it is not appropriate to terminate CU splitting early. To overcome this disadvantage, we incorporate the proposed CU early termination algorithm with an RD-cost limitation. If TSS_{total} is less than or equal to Th_{total} and the RD-cost of the best intra mode in the current CU depth (RD_{cur}) is less than or equal to the threshold of the RD-cost limitation (TH_{RD}), further CU splitting will be terminated early.

TABLE 3. Coding performance of the CU early termination algorithm when Th_{total} is set as 1000.

Sequences	BD-BR (%)	TS (%)
Kendo	0.83	49.6
Balloons	0.74	41.7
Poznan_Hall2	5.21	71.3
GT_Fly	0.60	56.4
Average	**1.85**	**54.8**

The range of the RD-cost varies for different QPs, so the threshold TH_{RD} should also be adaptively adjusted according to the QP variation. We collect the best RD-cost of each testing sequence under particular QP pairs and sort them from smallest to largest; the testing sequences and QP pairs are tabulated in Table 4. Furthermore, the RD costs on the order of 90% of every testing sequence under each specific QP pair, as illustrated in Fig. 17, are averaged and exploited to fit the regression curve portrayed in Fig. 18. The regression curve is formulated in (9), where QP denotes the texture QP

FIGURE 17. Illustration of selecting the RD-cost threshold.

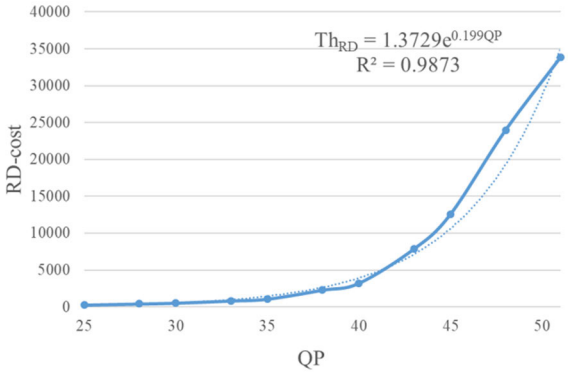

FIGURE 18. The regression curve of RD-cost and QP.

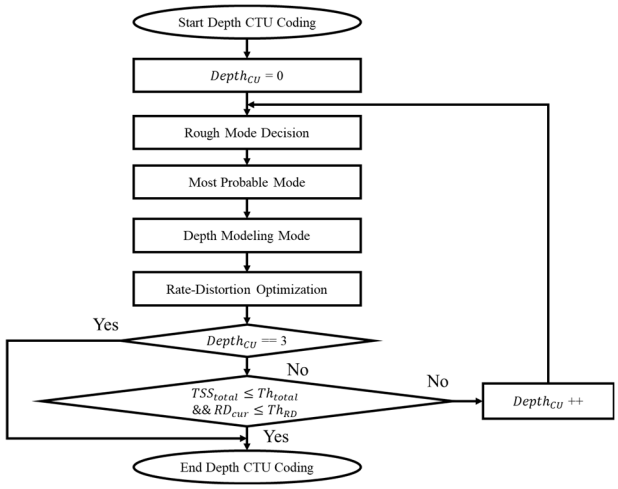

FIGURE 19. The flowchart of the fast CU early termination algorithm with RD-cost limitation.

in the QP pairs. Therefore, regardless of the QP, TH_{RD} will be adaptively fine-tuned, and we can obtain an appropriate value of TH_{RD} with (9). The flowchart of the complete fast CU early termination algorithm with RD-cost limitation is demonstrated in Fig. 19; $Depth_{CU}$ indicates the current CU depth.

$$Th_{RD} = 1.3729e^{0.199QP} \tag{9}$$

E. OVERALL ALGORITHM

The complete flowchart of the overall proposed algorithm is shown in Fig. 20 and includes the fast intra mode decision, fast DMM decision and fast CU early termination with the

TABLE 4. Testing sequences and QP pairs for the curve fitting of Th_{RD}.

Sequences	QP(color, depth)	Frames
Kendo, Balloons, Poznan_Hall2, GT_Fly	(25,34), (28,37), (30,39), (33,41), (35,42), (38,44), (40,45), (43,47), (45,48), (48,50),(51,51)	100

RD-cost limitation described in Section II.B to Section II.D. The detailed procedures are explained in the following.

Step 1: Start depth CTU encoding.
Step 2: Set current CU depth ($Depth_{CU}$) to 0.
Step 3: Calculate TSS_k by (1)-(2), Var_k by (4)-(6), and TSS_{total} by (8).
Step 4: As described in (3), if TSS_k is less than or equal to Th_{TSS}, continue to Step 5. Otherwise, go to Step 6.
Step 5: Only perform planar, DC, vertical, and horizontal intra prediction modes. In addition, reduce the number of RMD candidates to 3. Then, go to Step 7.
Step 6: Perform the unmodified conventional intra prediction modes.
Step 7: Add the MPM modes.
Step 8: As described in (7), if $(Var_1 + Var_2) - (Var_3 + Var_4)$ is less than or equal to Th_{var}, go to Step 10. Otherwise, continue to Step 9.
Step 9: Perform DMM prediction.
Step 10: Execute RDO. Then, if $Depth_{CU}$ is 3, go to Step 12. Otherwise, continue to Step 11.
Step 11: If TSS_{total} is less than or equal to Th_{total} and if RD_{cur} is less than or equal to Th_{RD} simultaneously, terminate CU splitting early and continue to Step 12. Otherwise, go back to Step 3 with $Depth_{CU}++$.
Step 12: Finish depth CTU encoding.

III. EXPERIMENTAL RESULTS

The proposed method is implemented on the 3D-HEVC reference software version 16.0 (HTM-16.0) [38] under all-intra configuration and three-view case. Four QP pairs are encoded, and all the setups of the experimental environment follow the common test condition (CTC) [39]. The setups of the testing environment are listed in Table 5. Eight testing sequences containing two resolutions (1024 × 768 and 1920 × 1088) are encoded. Detailed information on the testing sequences is itemized in Table 6. To investigate the effectiveness of the proposed fast coding algorithm, the time saving of depth map coding (DepthTS) related to HTM-16.0 is calculated by (10). The Bjøntegaard delta bitrate (BD-BR) [40], [41] is utilized to evaluate the coding efficiency. However, the depth map is for view synthesis or 3D displays instead of direct viewing. As a result, we compute the BD-BR of the synthesized view by the overall bitrate (color texture + depth map) and the quality of the synthesized view rather than only considering the depth map itself to evaluate

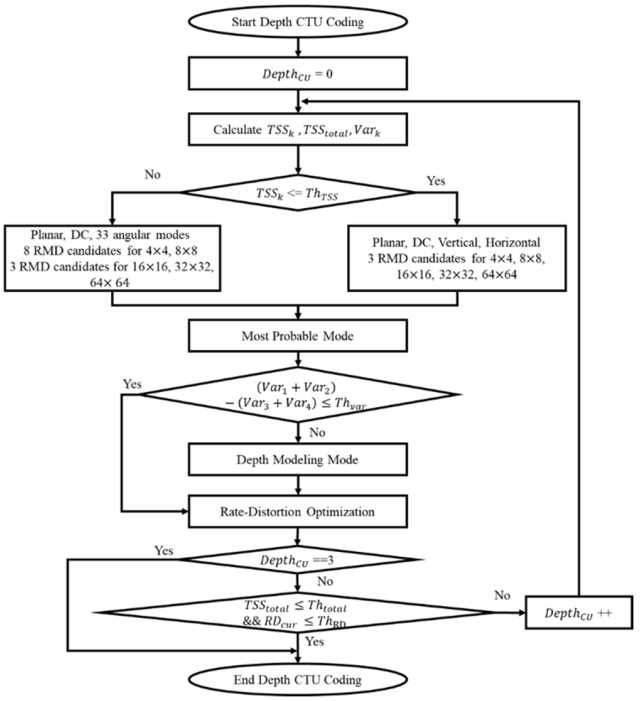

FIGURE 20. The complete flowchart of the overall proposed algorithm.

TABLE 5. Setups of the testing environment.

Testing Conditions	Settings
HTM version	HTM-16.0
Testing Case	Three-View Case with Depth Maps
Configurations	All-intra
QP(Color Texture, Depth Map)	(25,34),(30,39),(35,42),(40,45)
Intra Period	1

TABLE 6. Testing sequences.

Sequence	Resolution	Frame Rate	Frames	View
Kendo	1024×768	30	300	3-1-5
Balloons	1024×768	30	300	3-1-5
Newspaper	1024×768	30	300	4-2-6
Poznan_Street	1920×1088	25	250	4-5-3
Poznan_Hall2	1920×1088	25	200	6-7-5
Shark	1920×1088	30	300	5-1-9
Undo_Dancer	1920×1088	25	250	5-1-9
GT_Fly	1920×1088	25	250	5-9-1

the coding efficiency.

$$\text{Depth TS}\,(\%) = \frac{Depth\ Time_{HTM-16.0} - Depth\ Time_{proposed}}{Depth\ Time_{HTM-16.0}} \times 100\% \quad (10)$$

We compare the performance of the proposed algorithm to that of the algorithm proposed by Zhang *et al.* [26]. The BD-BR and depth time saving (TS) results are tabulated in Table 7. From Table 7, the proposed approach

TABLE 7. Performance comparison of BD-BR and depth time-saving.

Sequence	BD-BR(%)		Depth TS(%)	
	Zhang's [26]	Proposed	Zhang's [26]	Proposed
Kendo	0.43	0.17	38.23	48.04
Balloons	0.67	0.19	35.49	45.29
Newspaper	0.89	0.53	33.85	42.48
1024×768	**0.66**	**0.30**	**35.86**	**45.27**
Poznan_Street	0.29	0.22	39.67	59.03
Poznan_Hall2	0.75	0.71	48.33	72.25
Shark	0.33	0.22	34.16	58.92
UndoDancer	0.49	0.28	41.57	66.47
GT_Fly	0.21	0.25	43.14	56.16
1920×1088	**0.41**	**0.34**	**41.38**	**62.57**
Average	**0.51**	**0.32**	**39.31**	**56.08**

TABLE 8. Contributions of each individual part of the proposed algorithm.

Sequence	Fast Intra Mode Decision		Fast DMM Decision		Fast CU Early Termination Algorithm with RD-cost Limitation		Overall Algorithm	
	BD-BR (%)	Depth TS (%)	BD-BR (%)	Depth TS (%)	BD-BR (%)	Depth TS (%)	BD-BR (%)	Depth TS (%)
Kendo	0.07	17.25	0.05	8.19	0.03	42.23	0.17	48.04
Balloons	0.08	17.40	0.06	7.17	0.06	39.13	0.19	45.29
Newspaper	0.17	16.97	0.21	6.85	0.04	35.47	0.53	42.48
1024×768	**0.11**	**17.21**	**0.11**	**7.40**	**0.04**	**38.94**	**0.30**	**45.27**
Poznan_Street	0.07	19.70	0.10	10.73	0.02	53.56	0.22	59.03
Poznan_Hall2	0.11	21.73	0.35	12.18	0.06	68.52	0.71	72.25
Shark	0.06	19.44	0.07	11.77	0.00	52.64	0.22	58.92
UndoDancer	0.02	19.76	0.14	16.92	0.03	60.95	0.28	66.47
GT_Fly	0.04	18.98	0.08	10.82	0.00	52.19	0.25	56.16
1920×1088	**0.06**	**19.92**	**0.15**	**12.48**	**0.02**	**57.57**	**0.34**	**62.57**
Average	**0.08**	**18.90**	**0.13**	**10.58**	**0.03**	**50.58**	**0.32**	**56.08**

provides more significant depth time savings and outperforms previous work on each testing sequence. For the Poznan_Hall2 sequence, the time saving of the proposed algorithm even reach 72.25%, which is the greatest among all testing sequences. The averaged BD-BR performance of the proposed method is 0.32%, which is superior to that of [26] 0.51%. Compared to [26], approximately 16.77% of the depth coding time is further reduced by our scheme. In other words, we can diminish the depth coding time more significantly with negligible BD-BR degradation.

Most of the previous works only design a fast algorithm for the PU level. In this paper, we detect the boundary continuity and determine the boundary complexity in advance to reduce the computational complexity of conventional intra prediction and DMM prediction on the PU level. Moreover, we further combine the CU early termination algorithm with the RD-cost limitation on the CU level, which is why we can provide significant time-savings compared to previous work.

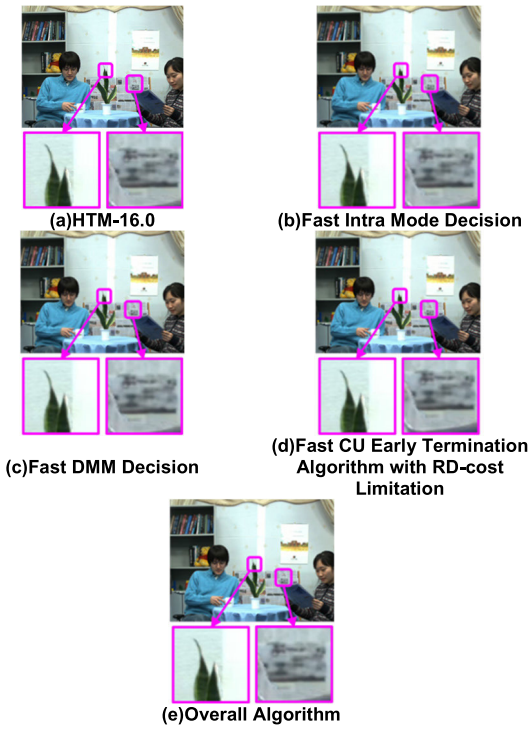

FIGURE 21. Subjective comparison of synthesized views and their zoomed regions generated by HTM-16.0 and the proposed criteria for the Newspaper sequence at the 2nd frame of the synthesized view 3.5.

Table 8 shows the contribution of each individual part of the proposed algorithm. Based on the boundary complexity of the PU, we conditionally simplify the intra modes to 4 kinds and reduce the number of rough mode decision candidates to 3. Approximately 18.90% of the coding time is saved, with only an 0.08% increase in the BD-BR on average. The fast DMM decision works more effectively for sequences with larger resolutions because they contain smoother areas. The fast CU early termination with RD-cost limitation, which has the largest contribution to time savings, determines whether to perform further CU splitting by an adaptively adjusted threshold with 50.58% time-saving. The proposed overall algorithm can considerably lessen the depth encoding time.

Fig. 21 and Fig. 22 demonstrate the subjective comparison of synthesized views by HTM-16.0 and the proposed criteria for the Newspaper and Undo_Dancer sequences, respectively. From the zoomed-in regions, it can be observed that the synthesized views generated by the proposed fast intra mode decision, fast DMM decision, fast CU early termination algorithm with RD-cost limitation and overall algorithm can maintain similar quality as those produced by HTM-16.0. In summary, the time-saving result of the overall proposed algorithm significantly outperforms that the previous work, and the proposed overall algorithm maintains great coding efficiency.

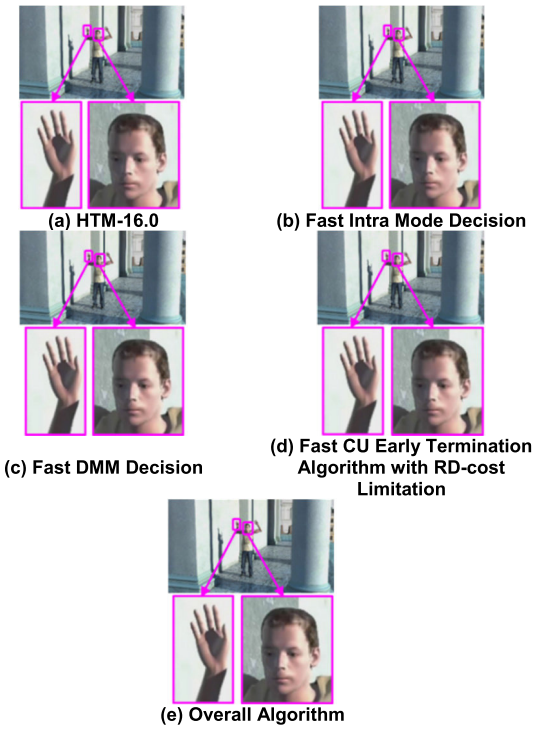

FIGURE 22. Subjective comparison of synthesized views and their zoomed regions generated by HTM-16.0 and the proposed criteria for the Undo_Dancer sequence at the 30th frame of the synthesized view 2.0.

IV. CONCLUSION

The 3D-HEVC encoder consumes considerable coding time during the PU mode decision and CU splitting. In addition, advanced techniques for depth map coding also bring about additional computational complexity. In this paper, we accelerate the depth map intra coding of 3D-HEVC based on boundary continuity. Three fast coding methods are proposed. First, the fast intra mode decision reduces the number of intra modes and RMD candidates based on boundary complexity. Second, the fast DMM decision effectively chooses whether to perform DMM prediction according to the difference of the boundary variances. Third, the fast CU early termination algorithm combines the RD-cost limitation to avoid unnecessary CU splitting in smooth areas. The experimental results show that we decrease the depth coding time by 56.08% with only a 0.32% increase in the BD-BR. The proposed algorithm outperforms the algorithm in the previous work with apparent time-saving improvements and maintains great coding efficiency.

REFERENCES

[1] Q. Zhang, Y. Wang, T. Wei, L. Huang, and R. Su, "A fast and efficient 3D-HEVC method for complexity reduction based on the correlations of inter-view, spatio-temporal, and texture-depth," *IEEE Access*, vol. 8, pp. 129075–129086, Jul. 2020.

[2] O. Stankiewicz, K. Wegner, and M. Domanski, "Study of 3D video compression using nonlinear depth representation," *IEEE Access*, vol. 7, pp. 31110–31122, Mar. 2019.

[3] O. Stankiewicz, M. Domanski, A. Dziembowski, A. Grzelka, D. Mieloch, and J. Samelak, "A free-viewpoint television system for horizontal virtual navigation," *IEEE Trans. Multimedia*, vol. 20, no. 8, pp. 2182–2195, Aug. 2018.

[4] P.-C. Huang, J.-R. Lin, G.-L. Li, K.-H. Tai, and M.-J. Chen, "Improved depth-assisted error concealment algorithm for 3D video transmission," *IEEE Trans. Multimedia*, vol. 19, no. 11, pp. 2625–2632, Nov. 2017.

[5] H. Roodaki, Z. Iravani, M. R. Hashemi, and S. Shirmohammadi, "A view-level rate distortion model for multi-view/3D video," *IEEE Trans. Multimedia*, vol. 18, no. 1, pp. 14–24, Jan. 2016.

[6] P. Merkle, K. Müller, and T. Wiegand, "Coding of depth signals for 3D video using wedgelet block segmentation with residual adaptation," in *Proc. IEEE Int. Conf. Multimedia Expo (ICME)*, San Jose, CA, USA, Jul. 2013, pp. 1–6.

[7] K. J. Oh, J. Lee, and D. S. Park, "Depth intra skip prediction for 3D video coding," in *Proc. Annu. Summit Conf. Signal Inf. Process. Assoc. (APSIPA ASC)*, Los Angeles, CA, USA, Dec. 2012, pp. 1–4.

[8] Y. Chen, G. Tech, K. Wegner, and S. Yea, *Test Model 11 of 3D-HEVC and MV-HEVC*, document JCT3V-K1003, Feb. 2015.

[9] A. Ortego and K. Ramchandran, "Rate-distortion methods for image and video compression," *IEEE Signal Process. Mag.*, vol. 15, no. 6, pp. 23–50, Nov. 1998.

[10] Y. Zhang, X. Yang, X. Liu, Y. Zhang, G. Jiang, and S. Kwong, "High-efficiency 3D depth coding based on perceptual quality of synthesized video," *IEEE Trans. Image Process.*, vol. 25, no. 12, pp. 5877–5891, Dec. 2016.

[11] L. Zhu, Y. Zhang, S. Wang, H. Yuan, S. Kwong, and H. H.-S. Ip, "Convolutional neural network-based synthesized view quality enhancement for 3D video coding," *IEEE Trans. Image Process.*, vol. 27, no. 11, pp. 5365–5377, Nov. 2018.

[12] S. Shahriyar, M. Murshed, M. Ali, and M. Paul, "Depth sequence coding with hierarchical partitioning and spatial-domain quantization," *IEEE Trans. Circuits Syst. Video Technol.*, vol. 30, no. 3, pp. 835–849, Mar. 2020.

[13] K.-L. Chung, Y.-H. Huang, C.-H. Lin, and J.-P. Fang, "Novel bitrate saving and fast coding for depth videos in 3D-HEVC," *IEEE Trans. Circuits Syst. Video Technol.*, vol. 26, no. 10, pp. 1859–1869, Oct. 2016.

[14] J. Lei, J. Duan, F. Wu, N. Ling, and C. Hou, "Fast mode decision based on grayscale similarity and inter-view correlation for depth map coding in 3D-HEVC," *IEEE Trans. Circuits Syst. Video Technol.*, vol. 28, no. 3, pp. 706–718, Mar. 2018.

[15] L. Shen, K. Li, G. Feng, P. An, and Z. Liu, "Efficient intra mode selection for depth-map coding utilizing spatiotemporal, inter-component and inter-view correlations in 3D-HEVC," *IEEE Trans. Image Process.*, vol. 27, no. 9, pp. 4195–4206, Sep. 2018.

[16] H. Hamout and A. Elyousfi, "Fast depth map intra coding for 3D video compression-based tensor feature extraction and data analysis," *IEEE Trans. Circuits Syst. Video Technol.*, vol. 30, no. 7, pp. 1933–1945, Jul. 2020.

[17] G. Sanchez, M. Saldanha, G. Balota, B. Zatt, M. Porto, and L. Agostini, "A complexity reduction algorithm for depth maps intra prediction on the 3D-HEVC," in *Proc. IEEE Vis. Commun. Image Process. Conf.*, Valletta, Malta, Dec. 2014, pp. 137–140.

[18] G. Sanchez, M. Saldanha, B. Zatt, M. Porto, and L. Agostini, "S-GMOF: A gradient-based complexity reduction algorithm for depth-maps intra prediction on 3D-HEVC," in *Proc. IEEE 6th Latin Amer. Symp. Circuits Syst. (LASCAS)*, Montevideo, Uruguay, Feb. 2015, pp. 1–4.

[19] M. Saldanha, B. Zatt, M. Porto, L. Agostini, and G. Sanchez, "Solutions for DMM-1 complexity reduction in 3D-HEVC based on gradient calculation," in *Proc. IEEE 7th Latin Amer. Symp. Circuits Syst. (LASCAS)*, Florianópolis, Brazil, Feb. 2016, pp. 211–214.

[20] C.-H. Fu, H.-B. Zhang, W.-M. Su, S.-H. Tsang, and Y.-L. Chan, "Fast wedgelet pattern decision for DMM in 3D-HEVC," in *Proc. IEEE Int. Conf. Digit. Signal Process. (DSP)*, Singapore, Jul. 2015, pp. 477–481.

[21] H.-B. Zhang, S.-H. Tsang, Y.-L. Chan, C.-H. Fu, and W.-M. Su, "Early determination of intra mode and segment-wise DC coding for depth map based on hierarchical coding structure in 3D-HEVC," in *Proc. Asia–Pacific Signal Inf. Process. Assoc. Annu. Summit Conf. (APSIPA)*, Hong Kong, Dec. 2015, pp. 374–378.

[22] R. H. Hong, M. J. Chen, and J. R. Lin, "Efficient DMM decision of depth intra coding in 3D-HEVC," in *Proc. 30th IPPR Conf. Comput. Vis., Graph., Image Process. (CVGIP)*, Taipei, Taiwan, Aug. 2017, pp. 1–4.

[23] Z. Gu, J. Zheng, N. Ling, and P. Zhang, "Fast bi-partition mode selection for 3D HEVC depth intra coding," in *Proc. IEEE Int. Conf. Multimedia Expo (ICME)*, Chengdu, China, Jul. 2014, pp. 1–6.

[24] C. S. Park, "Edge-based intra mode selection for depth-map coding in 3D-HEVC," *IEEE Trans. Image Process.*, vol. 24, no. 1, pp. 155–162, Jan. 2015.

[25] Q. Zhang, N. Li, L. Huang, and Y. Gan, "Effective early termination algorithm for depth map intra coding in 3D-HEVC," *Electron. Lett.*, vol. 50, no. 14, pp. 994–996, Jul. 2014.
[26] H.-B. Zhang, C.-H. Fu, Y.-L. Chan, S.-H. Tsang, and W.-C. Siu, "Probability-based depth intra-mode skipping strategy and novel VSO metric for DMM decision in 3D-HEVC," *IEEE Trans. Circuits Syst. Video Technol.*, vol. 28, no. 2, pp. 513–527, Feb. 2018.
[27] M. Saldanha, G. Sanchez, C. Marcon, and L. Agostini, "Fast 3D-HEVC depth map encoding using machine learning," *IEEE Trans. Circuits Syst. Video Technol.*, vol. 30, no. 3, pp. 850–861, Mar. 2020.
[28] J.-R. Lin, M.-J. Chen, C.-H. Yeh, Y.-C. Chen, L.-J. Kau, C.-Y. Chang, and M.-H. Lin, "Visual perception based algorithm for fast depth intra coding of 3D-HEVC," *IEEE Trans. Multimedia*, early access, Mar. 31, 2021, doi: 10.1109/TMM.2021.3070106.
[29] G. Shen, W.-S. Kim, A. Ortega, J. Lee, and H. Wey, "Edge-aware intra prediction for depth-map coding," in *Proc. IEEE Int. Conf. Image Process.*, Sep. 2010, pp. 3393–3396.
[30] G. Shen, W.-S. Kim, S. K. Narang, A. Ortega, J. Lee, and H. Wey, "Edge-adaptive transforms for efficient depth map coding," in *Proc. 28th Picture Coding Symp.*, Nagoya, Japan, Dec. 2010, pp. 566–569.
[31] V. Sanchez, "Sample-based edge prediction based on gradients for lossless screen content coding in HEVC," in *Proc. Picture Coding Symp. (PCS)*, Cairns, QLD, Australia, May 2015, pp. 134–138.
[32] S. Hu, R. A. Cohen, A. Vetro, and C.-C.-J. Kuo, "Screen content coding for HEVC using edge modes," in *Proc. IEEE Int. Conf. Acoust., Speech Signal Process.*, Vancouver, BC, Canada, May 2013, pp. 1714–1718.
[33] H. Chen, A. Saxena, and F. Fernandes, "Nearest-neighbor intra prediction for screen content video coding," in *Proc. IEEE Int. Conf. Image Process. (ICIP)*, Paris, France, Oct. 2014, pp. 3151–3155.
[34] Y.-C. Hsu, J.-R. Lin, and M.-J. Chen, "Fast DMM decision based on variance calculation for depth intra coding in 3D-HEVC," in *Proc. Taiwan Acad. Netw. Conf. (TANET)*, Taipei, Taiwan, Oct. 2017, pp. 387–390.
[35] Y.-C. Hsu, J.-R. Lin, M.-J. Chen, C.-H. Yeh, M.-H. Lin, and W.-C. Lu, "Acceleration of depth intra coding for 3D-HEVC by efficient early termination algorithm," in *Proc. IEEE Asia Pacific Conf. Circuits Syst. (APCCAS)*, Chengdu, China, Oct. 2018, pp. 127–130.
[36] Y.-C. Hsu, J.-R. Lin, M.-J. Chen, C.-H. Yeh, and R.-M. Weng, "Fast depth intra coding in 3D-HEVC based on boundary continuity," in *Proc. 11th Int. Conf. Digit. Image Process. (ICDIP)*, Guangzhou, China, May 2019, pp. 1–2.
[37] G. Sanchez, R. Cataldo, R. Fernandes, L. Agostini, and C. Marcon, "3D-HEVC depth maps intra prediction complexity analysis," in *Proc. IEEE Int. Conf. Electron., Circuits Syst. (ICECS)*, Monte Carlo, Monaco, Dec. 2016, pp. 348–351
[38] (2015). *3D-HEVC Reference Software Version 16.0 (HTM-16.0)*. [Online]. Available: https://hevc.hhi.fraunhofer.de/svn/svn_3DVCSoftware/tags/HTM-16.0/
[39] K. Müller and A. Vetro, *Common Test Conditions of 3DV Core Experiments*, document Rec. JCT3V-G1100, Joint Collaborative Team on 3D Video Coding Extension Development of ITU-T SG 16 WP 3 and ISO/IEC JTC 1/SC 29/WG 11, San Jose, CA, USA, Jan. 2014.
[40] G. Bjontegaard, *Calculation of Average PSNR Differences Between RD Curves*, document ITU-T SG16/Q6, VCEG-M33, Austin, TX, USA, Apr. 2001.
[41] G. Bjontegaard, *Improvements of the BD-PSNR Model*, document ITU-T SG16/Q6, VCEG-AI11, Berlin, Germany, Jul. 2008.

MEI-JUAN CHEN (Senior Member, IEEE) received the B.S., M.S., and Ph.D. degrees in electrical engineering from National Taiwan University, Taipei, Taiwan, in 1991, 1993, and 1997, respectively. From 1997 to 2000, she was an Assistant Professor with the Department of Electrical Engineering, National Dong Hwa University, Hualien, Taiwan, where she was an Associate Professor, from 2000 to 2005. Since August 2005, she has been a Professor with the Department of Electrical Engineering, National Dong Hwa University. From 2005 to 2006, she was also the Chair of the Department. Her research interests include image or video processing, video compression, motion estimation, error concealment, video transcoding, and artificial intelligence. She was a recipient of the Dragon Thesis Awards, in 1993 and 1997. She was a recipient of the 2005 K. T. Li Young Researcher Award from ACM Taipei/Taiwan Chapter for her contribution to video signal codec technique. This award was given annually to only one person under the age of 36, conducting research in Taiwan. She was also a recipient of the Outstanding Young Electrical Engineer Award from the Chinese Institute of Electrical Engineering, Taiwan, in 2006, the Best and Excellent Master/Ph.D. Thesis Supervision Awards from the Institute of Information and Computer Machinery, in 2006, 2015, and 2016, the Jun S. Huang Memorial Foundation Best Paper Awards, in 2005 and 2012, the IPPR society Best Paper Awards, in 2013, 2015, and 2016, the Best and Excellent Master Thesis Supervision Awards from Taiwan Institute of Electrical and Electronic Engineering, in 2011, 2014, 2015, and 2016, the Best Paper Award from National Symposium on Telecommunication, in 2014, the Best Paper Awards from Taiwan Academic Network Conference, in 2016 and 2017, the First Place of Best Paper Award from 2017 IEEE International Conference on Consumer Electronics—Taiwan, the Outstanding Electrical Engineering Professor Award from the Chinese Institute of Electrical Engineering, Taiwan, in 2020, and the Second Best Paper Award from the 2020 International Computer Symposium. She became a Fellow of IET, in 2019. She is an Associate Editor of the *EURASIP Journal on Advances in Signal Processing* and *International Journal of Electrical Engineering*.

JIE-RU LIN received the B.S., M.S., and Ph.D. degrees from the Department of Electrical Engineering, National Dong Hwa University, Hualien, Taiwan, in 2015, 2016, and 2020, respectively. From August 2018 to January 2019 and from August 2019 to January 2020, he was a Lecturer with the Department of Electrical Engineering, National Dong Hwa University. He is currently an Engineer with the Industrial Technology Research Institute, Taiwan. His research interests include video coding and point cloud compression. He was a recipient of the Best Paper Award from National Symposium on Telecommunication, in 2014, the Best Paper Award from IPPR Society and the Excellent Master Thesis Award from Taiwan Institute of Electrical and Electronic Engineering, in 2016, the Best Paper Awards from Taiwan Academic Network Conference, in 2016 and 2017, the First Place of Best Paper Award from 2017 IEEE International Conference on Consumer Electronics—Taiwan, in 2017, and the Second Best Paper Award from 2020 International Computer Symposium.

YU-CHIH HSU received the B.S. and M.S. degrees from the Department of Electrical Engineering, National Dong Hwa University, Hualien, Taiwan, in 2016 and 2019, respectively. His research interest focuses on the fast algorithm for the depth coding of 3D video.

YI-SHENG CIOU received the B.S. degree in electrical engineering from National Dong Hwa University, Hualien, Taiwan, in 2020, where he is currently pursuing the M.S. degree. His research interests include video coding algorithms in 3D-HEVC and H.266/VVC.

CHIA-HUNG YEH (Senior Member, IEEE) received the B.S. and Ph.D. degrees from the Department of Electrical Engineering, National Chung Cheng University, Chiayi, Taiwan, in 1997 and 2002, respectively. From August 2002 to December 2004, he was a Postdoctoral Fellow with the Department of Electrical Engineering-Systems, University of Southern California, Los Angeles, CA, USA. He was an Assistant Professor, from 2007 to 2010, an Associate Professor, from 2010 to 2013, and a Professor, from 2013 to 2017, with the Department of Electrical Engineering, National Sun Yat-sen University, Kaohsiung, Taiwan. He is currently a Distinguished Professor with National Taiwan Normal University, Taipei, Taiwan, and the Vice Dean of the College of Technology and Engineering. He has coauthored more than 250 technical international conference papers and journal articles and held 47 patents in the USA, Taiwan, and China. His research interests include multimedia, video communication, 3D reconstruction, video coding, image or video processing, and big data. He is an active TC Member of the IEEE Communication Society on Multimedia Communication, APSIPA, and IWAIT. He became a Fellow of IET, in 2017. He is also one of the Founding Member of ACM SIGMM Taiwan Chapter. He is on the Best Paper Award Committee of JVCI and APSIPA. He was a recipient of the 2007 Young Researcher Award of NSYSU, the 2011 Outstanding Young Electrical Engineer Award from the Chinese Institute of Electrical Engineering, the 2013 Distinguished Young Researcher Award of NSYSU, the 2013 IEEE MMSP Top 10% Paper Award, the 2014 IEEE GCCE Outstanding Poster Award, the 2015 APSIPA Distinguished Lecturer, the 2016 NAR Labs Technical Achievement Award, Superior Achievement Award, the 2017 IEEE SPS Tainan Section Chair, the 2017 Distinguished Professor Award of NTNU, the IEEE Outstanding Technical Achievement Award (IEEE Tainan Section), and the Second Best Paper Award from 2020 International Computer Symposium. He was an Associate Editor of the *Journal of Visual Communication and Image Representation*, *EURASIP Journal on Advances in Signal Processing*, and *APSIPA Transactions on Signal and Information Processing*.

MIN-HUI LIN received the B.S. degree in electrical engineering from National Kaohsiung University, Kaohsiung, Taiwan, in 2016, and the Ph.D. degree in electrical engineering from National Sun Yat-sen University, Kaohsiung, in 2021. She is currently a Senior Engineer with Qualcomm Inc., Taiwan. Her research interests include the deep learning for computer vision, 3D reconstruction, and multimedia applications. She was a recipient of the Best Oral Presentation Award from 2018 IEEE Asia-Pacific Conference on Circuits and Systems and the Second Best Paper Award from 2020 International Computer Symposium.

LIH-JEN KAU (Senior Member, IEEE) received the B.S. degree in control engineering, and the M.S. and Ph.D. degrees in electrical and control engineering from National Chiao Tung University, Hsinchu, Taiwan, in 1991, 1997, and 2008, respectively. From 1996 to 1998, he was with Chunghwa Telecom, Taipei, Taiwan, where he was a Senior Technician. He joined the Department of Computer and Communication Engineering, Dahan Institute of Technology, Hualien, Taiwan, as an Instructor, in August 1998. Since February 2006, he has been an Assistant Professor with the Dahan Institute of Technology. Since August 2009, he has been with the Department of Electronic Engineering (EE), National Taipei University of Technology (NTUT), Taipei, where he is currently an Associate Professor. His research interests include image or video coding and processing, healthcare and biomedical information technology, and autonomous vehicle system integration. He was a recipient of the 2003 ZyXEL Scholarship Award from ZyXEL Communications Corporation, Hsinchu, the Best Live Demonstration Award from the IEEE Biomedical Circuits and Systems Conference, in 2016, and the Best Paper Award from the IEEE International Conference of Intelligent Applied Systems on Engineering, in 2019.

CHUAN-YU CHANG (Senior Member, IEEE) received the Ph.D. degree in electrical engineering from National Cheng Kung University, Tainan, Taiwan, in 2000. From 2009 to 2011, he was the Chair of the Department of Computer Science and Information Engineering, National Yunlin University of Science and Technology (YunTech), Taiwan. From 2011 to 2019, he was the Dean of the Research and Development, the Director of the Incubation Center for Academia-Industry Collaboration and Intellectual Property, YunTech. He is currently the Deputy General Director of the Service Systems Technology Center, Industrial Technology Research Institute, Taiwan. He is also a Distinguished Professor with the Department of Computer Science and Information Engineering, YunTech. He has authored or coauthored more than 200 publications in journals and conference proceedings in his research fields, which include computational intelligence and their applications to medical image processing, automated optical inspection, emotion recognition, and pattern recognition. He is an IET Fellow, a Life Member of IPPR, and TAAI. He was the Program Co-Chair of TAAI 2007, CVGIP 2009, 2010–2019 International Workshop on Intelligent Sensors and Smart Environments, and the third International Conference on Robot, Vision and Signal Processing (RVSP 2015). He was the General Co-Chair of 2012 International Conference on Information Security and Intelligent Control, 2011–2013 Workshop on Digital Life Technologies, CVGIP 2017, WIC 2018, ICS 2018, and WIC 2019. From 2015 to 2017, he was the Chair of the IEEE Signal Processing Society Tainan Chapter and the Representative for Region 10 of IEEE SPS Chapters Committee. He is also the President of the Chinese Image Processing and Pattern Recognition Society, and the President of the Taiwan Association for Web Intelligence Consortium.